

The Yield-Strain and Shear-Band Direction in Amorphous Solids Under General Loading

Ashwin J.¹, Oleg Gendelman², Itamar Procaccia¹ and Carmel Shor¹

¹*Department of Chemical Physics, The Weizmann Institute of Science, Rehovot 76100, Israel*

²*Faculty of Mechanical Engineering, Technion, Haifa 32000, Israel.*

(Dated: September 27, 2018)

It is well known experimentally that well-quenched amorphous solids exhibit a plastic instability in the form of a catastrophic shear localization at a well defined value of the external strain. The instability may develop to a shear-band that in some cases is followed by a fracture. It is also known that the values of the yield-strain (and yield-stress), as well as the direction of the shear band with respect to the principal stress axis, vary considerably with variations in the external loading conditions. In this paper we present a microscopic theory of these phenomena for 2-dimensional athermal amorphous solids that are strained quasi-statically. We present analytic formulae for the yield-strains for different loading conditions, and well as for the angles of the shear bands. We explain that the external loading conditions determine the eigenvalues of the quadrupolar Eshelby inclusions which model the non-affine displacement field. These inclusions model elementary plastic events and determine both the yield-strain and the direction of the shear-band. We show that the angles of the shear bands with respect to the principal stress axis are limited theoretically between 30° and 60° . Available experimental data conform to this prediction.

I. INTRODUCTION

The physics of amorphous solids raises some problems that do not exist in perfect crystals. While it is well known that disorder brings about (Anderson) localization of eigenfunctions [1], it is commonly assumed that such localization is limited to eigenfunctions associated with high energies. Low-frequency eigenfunctions are believed to be spatially extended. This picture fails in amorphous solids that are subjected to an external strain. Here one finds that the lowest energy eigenfunction can become localized. This localization can take the form of a plastic event that changes the local organization of particles through the creation of essential non-affine displacement. Sometimes the plastic instability can exhibit itself as a system spanning event of shear localization along a line in 2-dimensional systems [2] and a plane in 3-dimensional systems [3]. These events are crucially important in limiting the toughness of technologically important materials like metallic glasses. These instabilities are the subject of this paper.

To be as precise as possible, we will deal in this paper with 2-dimensional systems (although the 3-dimensional extension is available [3]) which are athermal (at temperature $T = 0$) and strained quasi-statically [4]. We will consider systems which are good glass formers, containing N particles in a volume V , interacting via generic interaction potentials that are sufficiently smooth (with at least two continuous derivatives). The total energy can be written then in terms of the positions $\mathbf{r}_1, \mathbf{r}_2, \dots, \mathbf{r}_N$ of these particles, $U = U(\mathbf{r}_1, \mathbf{r}_2, \dots, \mathbf{r}_N)$. The Hessian matrix is defined as the second derivative [5]

$$H_{ij} \equiv \frac{\partial^2 U(\mathbf{r}_1, \mathbf{r}_2, \dots, \mathbf{r}_N)}{\partial \mathbf{r}_i \partial \mathbf{r}_j}. \quad (1)$$

The Hessian is real and symmetric, and therefore can be diagonalized. Excluding Goldstone modes whose eigen-

values are zero due to continuous symmetries, all the other eigenvalues are real and positive as long as the system is mechanically stable. In equilibrium, without any mechanical loading, the eigenfunctions associated with the large eigenvalues are localized due to Anderson localization, as it was mentioned above. However, all the eigenfunctions associated with the low eigenvalues (including all the excess modes that are typical to amorphous solids) are spatially extended. It had been a major discovery of the last decade that at small values of the external strain there appear “fundamental plastic events” in which the eigenvalues of Hessian matrix hit zero via a saddle node bifurcation, and simultaneously the associated eigenfunctions get localized [6]. This is a new mechanism for localization, different from the well known Anderson mechanism, and it is the basis for the understanding of plastic instabilities in amorphous solids. It had been shown that at low values of the external strains the spatial ranges of these plastic events are system-size independent [7], involving a small number of particles, of the order of 100. The displacement fields associated with fundamental plastic events are reliably modeled by Eshelby inclusions (see below for details). It had been a more recent discovery that at higher values of the external strains these fundamental plastic events can organize in highly correlated lines in 2-dimensional system or in planes in 3 dimensional systems [2, 3]. These highly correlated *densities* of Eshelby inclusions are the microscopic manifestation of the shear localization.

The key idea of the recent work on the shear localization is that at $T = 0$ with quasi-static loading the preferred spatial organization of the density of Eshelby inclusions could be found by minimizing their total energy in the strained system. In Refs. [2, 3] the theory was worked out for simple external shear in both 2 and 3 dimensions. It was found that in the case of a pure external shear the shear-localization is realized by organizing the

inclusions on a line (plane) in 2 (3) dimensions that are precisely at 45° with respect to the principal stress axis. An additional important result is an analytic prediction for the yield-strain (where shear localization occurs for the first time) in terms of the properties of the Eshelby solution for the fundamental plastic event (a single inclusion).

It is well known however that for other loading conditions, e.g. uniaxial tension or compression, the value of the yield strain as well as the direction of the shear band can vary considerably [8], indicating that the pure shear is a special case. It was reported recently in [9] that the difference can be related to the more general form of the Eshelby inclusion which models the fundamental plastic instability at different loading conditions. The aim of the present paper is to offer the theory in sufficient detail and to work out analytic predictions of the yield strain. The calculations involved are straightforward but sometimes cumbersome, and we make an effort to offer them in an optimally didactic way in the sequel.

In Sect. II we present results for AQS numerical simulations in uniaxial compression and extension to provide us with data on yield strains and directions of shear bands. We find the well known asymmetry in both measures. In Sect. III we begin to develop the general theory for 2-dimensional Eshelby inclusions that is appropriate for the most general loading conditions. In Sect. IV we compute the all-important energy of \mathcal{N} inclusions, and minimize it to find the preferred organizations and the resulting angle of the shear band. On the basis of this calculation we offer in Sect. V an analytic prediction for the yield strain. The final section VI provides a short summary and a discussion.

The reader should note that throughout this paper we will reserve the Greek letters $\alpha, \beta, \gamma, \dots$ for tensor subscripts, while the Latin letters i, j, k, \dots will be used for particles and Eshelby inclusions.

II. NUMERICAL SIMULATIONS

To prepare data for the present analysis we have performed two-dimensional (2D) Molecular Dynamics simulations on a binary system which is known to be a good glass former and has a quasi-crystalline ground state [10, 11]. Each atom in the system is labeled as either “small” (S) or “large” (L) and all the particles interact via Lennard-Jones (LJ) potential. All distances $|\mathbf{r}_i - \mathbf{r}_j|$ are normalized by λ_{SL} , the distance at which the LJ potential between the two species becomes zero and the energy is normalized by ϵ_{SL} which is the interaction energy between the two species. Temperature was measured in units of ϵ_{SL}/k_B where k_B is Boltzmann’s constant. For detailed information on the model potential and its properties, we refer the reader to Ref [10]. The number of particles in our simulations is 10000 at a number density $n = 0.985$ with a particle ratio $N_L/N_s = (1 + \sqrt{5})/4$. The mode coupling temperature T_{MCT} for this system is

known to be close to 0.325. The mass of all particles is $m_0 = 1$ and time is normalized to $t_0 = \sqrt{\epsilon_{SL}\lambda_{SL}^2/m_0}$. For the sake of computational efficiency, the interaction potential is smoothly truncated to zero along with its first two derivatives at a cut-off distance $r_c = 2.5$. To prepare the glasses, we first start from a well equilibrated liquid at a high temperature of $T = 1.2$ which is supercooled to $T = 0.35$ at relatively fast quenching rate of 3.4×10^{-3} . Then, we equilibrated these supercooled liquids for times greater than $20\tau_{rel}$, where τ_{rel} is the time taken for the self intermediate scattering function to approach 1% of its initial value. Lastly, following this equilibration, we quenched these supercooled liquids deep into the glassy regime at a temperature of $T = 0.01$ at a reduced quench rate of 3.2×10^{-6} . Following this quench we took the glass to mechanical equilibrium (nearest energy minima) by a conjugate gradient energy minimization. After that we start loading our glasses under athermal quasi-static conditions. Two different loading protocols were applied, one is uniaxial compression and the other - uniaxial extension. The simulations were followed until the yield strain γ_Y and slightly above to ascertain the angle of the shear band formed. The shear band is marked on the sample by coloring particles using their values of D_{min}^2 [12]. We use a binary coloring scheme which means that when a given particle i has $D_{min}^2(i) > \lambda_{SL}^2$, it is colored black, else it is colored white.

We note the asymmetry in γ_Y , close to 5.5% for compression and 3.5% for extension, and the asymmetry in angles, 46° and 54° respectively. The theory outlined in this paper provides analytic formulae for both measures, cf Eqs. (74) and (78).

III. THEORY OF THE FUNDAMENTAL PLASTIC EVENT

In the past, phenomenological models were applied to this problem [13–17], but a microscopic approach was lacking. In this section we present the theory of 2-dimensional Eshelby inclusions for the general loading conditions.

A. Two Dimensional Circular Inclusion

Consider an elastic solid having a volume V and surface area S [Fig. 3]. The material will be assumed to be homogeneous with an elastic stiffness tensor given by $\mathcal{C}_{\alpha\beta\gamma\delta}$. Let a sub-volume V_0 with surface area S_0 undergo a uniform permanent (inelastic) deformation, such as a structural phase transformation. The material inside V_0 is referred to as an inclusion and the material outside is called the matrix. If we could remove this inclusion from its surrounding material then it would attain a state of a uniform strain and zero stress. Such a stress free strain is referred to as the eigen-strain $\epsilon_{\alpha\beta}^*$.

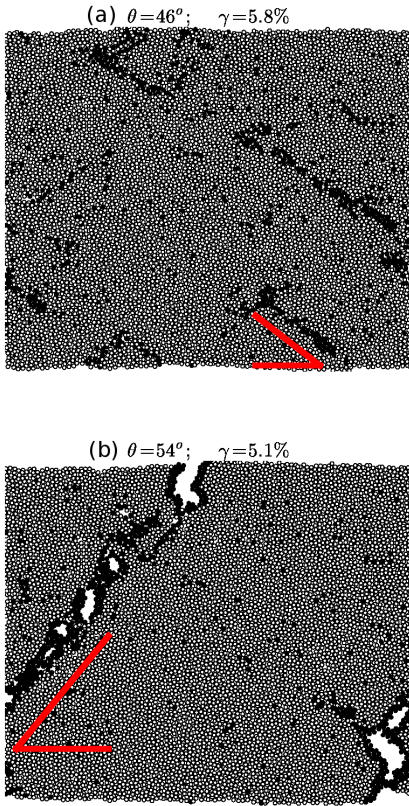


FIG. 1. Color Online: The shear band that occurs in a 2-dimensional amorphous solid upon uniaxial compression (a) and extension (b). The angle with respect to the principal stress component measured in compression is $46^\circ \pm 1^\circ$, whereas in the extension it is $54^\circ \pm 1^\circ$.

The eigen stress is then given by $\sigma_{\alpha\beta}^* = \mathcal{C}_{\alpha\beta\gamma\delta} \epsilon_{\gamma\delta}^*$.

In reality, the inclusion is surrounded by the matrix. Therefore, it is not able to reach the state of zero stress. Instead, both the inclusion and the matrix will deform and experience an elastic stress field. The Eshelby's transformed inclusion problem [18] is to solve the stress, strain and displacement fields both in the inclusion and in the matrix.

We consider a 2D circular inclusion that has been strained into an ellipse using an eigen-strain $\epsilon_{\alpha\beta}^*$ and which allows for a volume change ($\epsilon_{\nu\nu}^* \neq 0$). A general expression for such a tensor can be written in terms of a unit eigenvectors (\hat{n}, \hat{k}) and corresponding eigenvalues (ζ_n, ζ_k) as follows:

$$\epsilon_{\alpha\beta}^* = \zeta_n \hat{n}_\alpha \hat{n}_\beta + \zeta_k \hat{k}_\alpha \hat{k}_\beta \quad (2)$$

Using orthogonality of the eigen directions: $\hat{n}_\alpha \hat{n}_\beta + \hat{k}_\alpha \hat{k}_\beta = \delta_{\alpha\beta}$, we get:

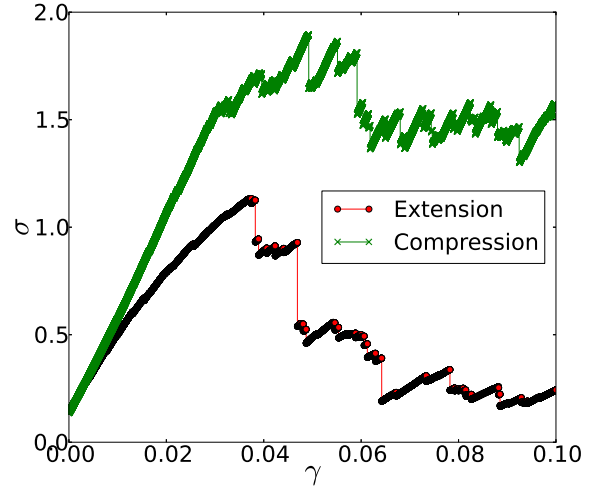


FIG. 2. Color Online: A typical stress strain curve obtained under AQS conditions for uniaxial tension (lower curve: red filled circles) and compression (upper curve: green crosses). The nonlinear response is clearly asymmetric with yield strain γ_Y being $\approx 5.5\%$ for compression and 3.5% for extension respectively. In Sect. V, we provide an analytic formula for yield strain which predicts this asymmetry to a very high degree of accuracy.

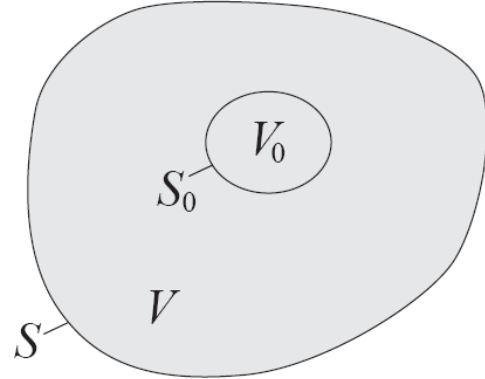


FIG. 3. Cartoon showing an elastic medium of volume V and surface area S . Inside the medium a small ellipsoidal region (volume V_0 and surface area S_0) undergoes an irreversible (plastic) deformation. The material inside V_0 is called as the *inclusion* and the material outside is referred to as the *matrix*.

$$\begin{aligned} \epsilon_{\alpha\beta}^* &= \frac{(\zeta_n - \zeta_k)}{2} (2\hat{n}_\alpha \hat{n}_\beta - \delta_{\alpha\beta}) + \frac{(\zeta_n + \zeta_k)}{2} \delta_{\alpha\beta} \\ &= \epsilon_{\alpha\beta}^{*,0} + \epsilon_{\alpha\beta}^{*,T} \end{aligned} \quad (3)$$

where the traceless part $\epsilon_{\alpha\beta}^{*,0}$ and the nonzero trace part

$\epsilon_{\alpha\beta}^{*,T}$ are given as

$$\begin{aligned}\epsilon_{\alpha\beta}^{*,0} &= \frac{(\zeta_n - \zeta_k)}{2}(2\hat{n}_\alpha\hat{n}_\beta - \delta_{\alpha\beta}) \\ \epsilon_{\alpha\beta}^{*,T} &= \frac{(\zeta_n + \zeta_k)}{2}\delta_{\alpha\beta}\end{aligned}\quad (4)$$

We also assume that the system is acted upon by a homogeneous strain $\epsilon_{\alpha\beta}^\infty$ that acts globally (which in our case also triggers the local transformation of the inclusion). This strained ellipsoidal inclusion feels a traction exerted by the surrounding elastic medium resulting in a constrained strain $\epsilon_{\alpha\beta}^c$ in the inclusion and also exerts a traction at the inclusion-matrix interface resulting in the originally unstrained surroundings developing a constrained strain field $\epsilon_{\alpha\beta}^c(\mathbf{X})$.

The eigen-strain $\epsilon_{\alpha\beta}^*$ in the inclusion is related to the constrained strain $\epsilon_{\alpha\beta}^c$ via the fourth order Eshelby tensor $\mathcal{S}_{\alpha\beta\gamma\delta}$:

$$\epsilon_{\alpha\beta}^c = \mathcal{S}_{\alpha\beta\gamma\delta}\epsilon_{\gamma\delta}^* \quad (5)$$

Now for an inclusion of arbitrary shape the constrained strain $\epsilon_{\alpha\beta}^c$, both the stress $\sigma_{\alpha\beta}^c$ and the displacement field $\mathbf{u}^c(\mathbf{X})$ inside the inclusion are in general functions of space. For ellipsoidal inclusions, however, it was shown by Eshelby [18, 19] that the Eshelby tensor and the constrained stress and strain fields inside the inclusion become independent of space. We work here with a circular inclusion which is a special case of an ellipse and hence for such an inclusion, the Eshelby tensor $\mathcal{S}_{\alpha\beta\gamma\delta}$ reads [20]

$$\mathcal{S}_{\alpha\beta\gamma\delta} = \frac{(\lambda - \mu)}{4(\lambda + 2\mu)}\delta_{\alpha\beta}\delta_{\gamma\delta} + \frac{(\lambda + 3\mu)}{4(\lambda + 2\mu)}(\delta_{\alpha\delta}\delta_{\beta\gamma} + \delta_{\alpha\gamma}\delta_{\beta\delta}) \quad (6)$$

where λ, μ are Lamé coefficients. Plugging Eq (6) in Eq (5), we get

$$\epsilon_{\alpha\beta}^c = \frac{(\lambda + \mu)}{(\lambda + 2\mu)}\epsilon_{\alpha\beta}^{*,T} + \frac{(\lambda + 3\mu)}{2(\lambda + 2\mu)}\epsilon_{\alpha\beta}^{*,0} \quad (7)$$

The total stress, strain and displacement field inside the circular inclusion are then given by

$$\begin{aligned}\epsilon_{\alpha\beta}^I &= \epsilon_{\alpha\beta}^c + \epsilon_{\alpha\beta}^\infty \\ \sigma_{\alpha\beta}^I &= \sigma_{\alpha\beta}^c - \sigma_{\alpha\beta}^* + \sigma_{\alpha\beta}^\infty \equiv C_{\alpha\beta\gamma\delta}(\epsilon_{\gamma\delta}^c - \epsilon_{\gamma\delta}^* + \epsilon_{\gamma\delta}^\infty) \\ \mathbf{u}_{\alpha}^I &= \mathbf{u}_{\alpha}^c + \mathbf{u}_{\alpha}^\infty = (\epsilon_{\alpha\beta}^c + \epsilon_{\alpha\beta}^\infty)X_{\beta}\end{aligned}\quad (8)$$

where the superscript I indicates the inclusion. The eigen stress $\sigma_{\alpha\beta}^*$ is related to the eigen strain $\epsilon_{\alpha\beta}^*$ as

$$\begin{aligned}\sigma_{\alpha\beta}^* &= C_{\alpha\beta\gamma\delta}\epsilon_{\gamma\delta}^* \\ &= 2\mu\epsilon_{\alpha\beta}^* + \lambda\epsilon_{\eta\eta}^*\delta_{\alpha\beta}\end{aligned}\quad (9)$$

where we have used the following definition of the fourth order elastic stiffness tensor $C_{\alpha\beta\gamma\delta}$ for an isotropic elastic medium:

$$C_{\alpha\beta\gamma\delta} = \lambda\delta_{\alpha\beta}\delta_{\gamma\delta} + \mu(\delta_{\alpha\gamma}\delta_{\beta\delta} + \delta_{\alpha\delta}\delta_{\beta\gamma}). \quad (10)$$

The stress in the inclusion can now be written down in terms of the independent variables using equations (9) as

$$\sigma_{\alpha\beta}^I = 2\mu\left(\epsilon_{\alpha\beta}^c - \epsilon_{\alpha\beta}^* + \epsilon_{\alpha\beta}^\infty\right) + \lambda\left(\epsilon_{\eta\eta}^c - \epsilon_{\eta\eta}^* + \epsilon_{\eta\eta}^\infty\right)\delta_{\alpha\beta} \quad (11)$$

B. Constrained Fields in the Matrix

In the surrounding elastic matrix, the stress, strain and displacement fields are all explicit functions of space and can be written as

$$\begin{aligned}\epsilon_{\alpha\beta}^m(\mathbf{X}) &= \epsilon_{\alpha\beta}^c(\mathbf{X}) + \epsilon_{\alpha\beta}^\infty \\ \sigma_{\alpha\beta}^m(\mathbf{X}) &= \sigma_{\alpha\beta}^c(\mathbf{X}) + \sigma_{\alpha\beta}^\infty \\ \mathbf{u}_{\alpha\beta}^m(\mathbf{X}) &= \mathbf{u}_{\alpha\beta}^c(\mathbf{X}) + \mathbf{u}_{\alpha\beta}^\infty\end{aligned}\quad (12)$$

The displacement field $u_{\alpha}^c(\mathbf{X})$ in the isotropic elastic medium will satisfy the Lamé-Navier equation (without any body forces) [21]

$$(\mu + \lambda)\frac{\partial^2 u_{\gamma}^c}{\partial X_{\alpha}\partial X_{\gamma}} + \mu\frac{\partial^2 u_{\alpha}^c}{\partial X_{\beta}\partial X_{\beta}} = 0 \quad (13)$$

The constrained fields in the inclusion will supply the boundary conditions for the displacement field in the matrix at the inclusion boundary. Also as $r \rightarrow \infty$, the constrained displacement field will vanish.

All solutions of Eq. (13) also obey the higher order bi-harmonic equation

$$\frac{\partial^4 u_{\alpha}^c}{\partial X_{\beta}\partial X_{\beta}\partial X_{\lambda}\partial X_{\lambda}} = \nabla^4 u_{\alpha}^c = 0 \quad (14)$$

Thus our objective is to construct from the radial solutions of the bi-Laplacian equation Eq. (14) derivatives which also satisfy Eq. (13). Note that the bi-Laplacian equation is only a necessary (but not a sufficient) condition for the solutions and Eq. (13) still needs to be satisfied.

C. Solution of the Lamé-Navier Equation

From the foregoing section, we note that the constrained displacement field due to the Eshelby solution is given as

$$\begin{aligned}u_{\alpha}^c &= \epsilon_{\alpha\beta}^c X_{\beta} \\ &= \left[\frac{(\lambda + \mu)}{(\lambda + 2\mu)}\epsilon_{\alpha\beta}^{*,T} + \frac{(\lambda + 3\mu)}{2(\lambda + 2\mu)}\epsilon_{\alpha\beta}^{*,0} \right] X_{\beta} \\ &= \frac{(\zeta_n + \zeta_k)(\lambda + \mu)}{2(\lambda + 2\mu)}X_{\alpha} + \frac{(\lambda + 3\mu)}{2(\lambda + 2\mu)}\epsilon_{\alpha\beta}^{*,0}X_{\beta}\end{aligned}\quad (15)$$

where we take the expression for $\epsilon_{\alpha\beta}^c$ from Eq. (7). We will look for linear combinations of the derivatives of the radial solutions of the bi-harmonic equation (14) which are linear in the eigen-strain and go to zero at large distance. In addition the terms must transform as a vector field. Let $\mathbf{u}^{c,T}$ and $\mathbf{u}^{c,0}$ be the solutions to the Lamé-Navier equations. We then have:

$$\begin{aligned} (\mu + \lambda) \frac{\partial^2 u_\gamma^{c,T}}{\partial X_\alpha \partial X_\gamma} + \mu \frac{\partial^2 u_\alpha^{c,T}}{\partial X_\beta \partial X_\beta} &= 0 \\ (\mu + \lambda) \frac{\partial^2 u_\gamma^{c,0}}{\partial X_\alpha \partial X_\gamma} + \mu \frac{\partial^2 u_\alpha^{c,0}}{\partial X_\beta \partial X_\beta} &= 0 \end{aligned} \quad (16)$$

Using the radial solutions of the Lamé-Navier equation we can construct the following combinations which transform as a vector and also go to zero as $r \rightarrow \infty$.

$$u_\alpha^{c,T} = A \epsilon_{\alpha\beta}^{*,T} \frac{\partial \ln r}{\partial X_\beta} + B \epsilon_{\beta\gamma}^{*,T} \frac{\partial^3 \ln r}{\partial X_\alpha \partial X_\beta \partial X_\gamma} + C \epsilon_{\beta\gamma}^{*,T} \frac{\partial^3 (r^2 \ln r)}{\partial X_\alpha \partial X_\beta \partial X_\gamma} \quad (17)$$

and

$$u_\alpha^{c,0} = A' \epsilon_{\alpha\beta}^{*,0} \frac{\partial \ln r}{\partial X_\beta} + B' \epsilon_{\beta\gamma}^{*,0} \frac{\partial^3 \ln r}{\partial X_\alpha \partial X_\beta \partial X_\gamma} + C' \epsilon_{\beta\gamma}^{*,0} \frac{\partial^3 (r^2 \ln r)}{\partial X_\alpha \partial X_\beta \partial X_\gamma} \quad (18)$$

Using the identities

$$\frac{\partial^2 \ln r}{\partial X_\beta \partial X_\beta} = 0; \quad \frac{\partial^2 (r^2 \ln r)}{\partial X_\beta \partial X_\beta} = 4 \ln r + 4 \quad (19)$$

we see from Eq (17)

$$\frac{\partial^2 u_\alpha^{c,T}}{\partial X_\beta \partial X_\beta} = 4C \epsilon_{\eta\lambda}^{*,T} \frac{\partial^3 \ln r}{\partial X_\alpha \partial X_\eta \partial X_\lambda} \quad (20)$$

and similarly

$$\frac{\partial^2 u_\gamma^{c,T}}{\partial X_\alpha \partial X_\gamma} = (A + 4C) \epsilon_{\eta\lambda}^{*,T} \frac{\partial^3 \ln r}{\partial X_\alpha \partial X_\eta \partial X_\lambda} \quad (21)$$

Plugging Eq (20), (21) into Eq (16), we get

$$C = -\frac{A(\lambda + \mu)}{4(\lambda + 2\mu)} \quad (22)$$

We can now rewrite Eq (17) as

$$u_\alpha^{c,T} = A \epsilon_{\alpha\beta}^{*,T} \frac{\partial \ln r}{\partial X_\beta} + B \epsilon_{\beta\gamma}^{*,T} \frac{\partial^3 \ln r}{\partial X_\alpha \partial X_\beta \partial X_\gamma} - \frac{A(\lambda + \mu)}{4(\lambda + 2\mu)} \epsilon_{\beta\gamma}^{*,T} \frac{\partial^3 (r^2 \ln r)}{\partial X_\alpha \partial X_\beta \partial X_\gamma} \quad (23)$$

We now compute the following identities

$$\begin{aligned} \frac{\partial \ln r}{\partial X_\beta} &= \frac{X_\beta}{r^2} \\ \frac{\partial^3 \ln r}{\partial X_\alpha \partial X_\beta \partial X_\gamma} &= \frac{-2r^2(X_\alpha \delta_{\beta\gamma} + X_\beta \delta_{\alpha\gamma} + X_\gamma \delta_{\alpha\beta}) + 8X_\alpha X_\beta X_\gamma}{r^6} \\ \frac{\partial^3 (r^2 \ln r)}{\partial X_\alpha \partial X_\beta \partial X_\gamma} &= \frac{2r^2(X_\alpha \delta_{\beta\gamma} + X_\beta \delta_{\alpha\gamma} + X_\gamma \delta_{\alpha\beta}) - 4X_\alpha X_\beta X_\gamma}{r^4} \end{aligned} \quad (24)$$

Using these identities, we can now write down Eq (23) as

$$u_\alpha^{c,T} = A \epsilon_{\alpha\beta}^{*,T} \frac{X_\beta}{r^2} - \left[\frac{2B}{r^4} + \frac{A(\lambda + \mu)}{2(\lambda + 2\mu)r^2} \right] \epsilon_{\beta\gamma}^{*,T} (X_\alpha \delta_{\beta\gamma} + X_\beta \delta_{\alpha\gamma} + X_\gamma \delta_{\alpha\beta}) + \left[\frac{8B}{r^6} + \frac{A(\lambda + \mu)}{(\lambda + 2\mu)r^4} \right] \epsilon_{\beta\gamma}^{*,T} X_\alpha X_\beta X_\gamma \quad (25)$$

and similarly

$$u_\alpha^{c,0} = A' \epsilon_{\alpha\beta}^{*,0} \frac{X_\beta}{r^2} - \left[\frac{2B'}{r^4} + \frac{A'(\lambda + \mu)}{2(\lambda + 2\mu)r^2} \right] \epsilon_{\beta\gamma}^{*,0} (X_\alpha \delta_{\beta\gamma} + X_\beta \delta_{\alpha\gamma} + X_\gamma \delta_{\alpha\beta}) + \left[\frac{8B'}{r^6} + \frac{A'(\lambda + \mu)}{(\lambda + 2\mu)r^4} \right] \epsilon_{\beta\gamma}^{*,0} X_\alpha X_\beta X_\gamma \quad (26)$$

Now using Eq. (4), we can rewrite equations (25) and (26) as

$$u_\alpha^{c,T} = \frac{(\zeta_n + \zeta_k) \mu A X_\alpha}{2(\lambda + 2\mu) r^2} \quad (27)$$

$$u_\alpha^{c,0} = \left(\frac{A' \mu}{(\lambda + 2\mu) r^2} - \frac{4B'}{r^4} \right) \epsilon_{\alpha\beta}^{*,0} X_\beta + \left(\frac{8B'}{r^6} + \frac{A'(\lambda + \mu)}{(\lambda + 2\mu) r^4} \right) \epsilon_{\beta\gamma}^{*,0} X_\alpha X_\beta X_\gamma \quad (28)$$

The complete solution for the displacement field in the matrix is then given as

$$\begin{aligned} u_\alpha^c &= u_\alpha^{c,T} + u_\alpha^{c,0} \\ &= \frac{(\zeta_n + \zeta_k)\mu AX_\alpha}{2(\lambda + 2\mu)r^2} + \left(\frac{A'\mu}{(\lambda + 2\mu)r^2} - \frac{4B'}{r^4} \right) \epsilon_{\alpha\beta}^{*,0} X_\beta + \left(\frac{8B'}{r^6} + \frac{A'(\lambda + \mu)}{(\lambda + 2\mu)r^4} \right) \epsilon_{\beta\gamma}^{*,0} X_\alpha X_\beta X_\gamma \end{aligned} \quad (29)$$

Now at $r = a$ (the inclusion boundary), the form of solution (29) must match with the Eshelby solution (15). This implies,

$$A = \frac{a^2(\lambda + \mu)}{\mu}, \quad A' = a^2, \quad B' = -\frac{a^4(\lambda + \mu)}{8(\lambda + 2\mu)} \quad (30)$$

Plugging equation (30) into Eq. (29), we get:

$$u_\alpha^c = \frac{(\lambda + \mu)}{2(\lambda + 2\mu)} \left(\frac{a^2}{r^2} \right) \left[(\zeta_n + \zeta_k) X_\alpha + \left(\frac{2\mu}{\lambda + \mu} + \frac{a^2}{r^2} \right) \epsilon_{\alpha\beta}^{*,0} X_\beta + 2 \left(1 - \frac{a^2}{r^2} \right) \epsilon_{\beta\gamma}^{*,0} \frac{X_\alpha X_\beta X_\gamma}{r^2} \right] \quad (31)$$

Noting that

$$\epsilon_{\alpha\beta}^{*,0} X_\beta = \frac{(\zeta_n - \zeta_k)}{2} (2\hat{n}_\alpha (\hat{\mathbf{n}} \cdot \mathbf{X}) - X_\alpha) \quad (32)$$

and

$$\epsilon_{\beta\gamma}^{*,0} X_\alpha X_\beta X_\gamma = \frac{(\zeta_n - \zeta_k)}{2} (2(\hat{\mathbf{n}} \cdot \mathbf{X})^2 - r^2) X_\alpha \quad (33)$$

we find that Eq. (31) finally becomes

$$\begin{aligned} \mathbf{u}^c(\mathbf{X}) &= \frac{(\zeta_n - \zeta_k)(\lambda + \mu)}{4(\lambda + 2\mu)} \left(\frac{a^2}{r^2} \right) \left[2 \frac{(\zeta_n + \zeta_k)}{(\zeta_n - \zeta_k)} \mathbf{X} + \left(\frac{2\mu}{\lambda + \mu} + \frac{a^2}{r^2} \right) (2(\hat{\mathbf{n}} \cdot \mathbf{X})\hat{\mathbf{n}} - \mathbf{X}) \right. \\ &\quad \left. + 2 \left(1 - \frac{a^2}{r^2} \right) (2(\hat{\mathbf{n}} \cdot \hat{\mathbf{r}})^2 - 1) \mathbf{X} \right] \end{aligned} \quad (34)$$

where $\hat{\mathbf{r}} = \frac{\mathbf{X}}{r}$. The Cartesian components of Eq. (34) used for visualizing the displacement field in space are given below:

$$\begin{aligned} u_x^c(\mathbf{X}) &= \frac{(\zeta_n - \zeta_k)(\lambda + \mu)}{4(\lambda + 2\mu)} \left(\frac{a^2}{r^2} \right) \left[2 \frac{(\zeta_n + \zeta_k)}{(\zeta_n - \zeta_k)} x + \left(\frac{2\mu}{\lambda + \mu} + \frac{a^2}{r^2} \right) (x \cos 2\phi + y \sin 2\phi) \right. \\ &\quad \left. + 2 \left(1 - \frac{a^2}{r^2} \right) \left(\frac{(x^2 - y^2) \cos 2\phi + 2xy \sin 2\phi}{r^2} \right) x \right] \\ u_y^c(\mathbf{X}) &= \frac{(\zeta_n - \zeta_k)(\lambda + \mu)}{4(\lambda + 2\mu)} \left(\frac{a^2}{r^2} \right) \left[2 \frac{(\zeta_n + \zeta_k)}{(\zeta_n - \zeta_k)} y + \left(\frac{2\mu}{\lambda + \mu} + \frac{a^2}{r^2} \right) (x \sin 2\phi - y \cos 2\phi) \right. \\ &\quad \left. + 2 \left(1 - \frac{a^2}{r^2} \right) \left(\frac{(x^2 - y^2) \cos 2\phi + 2xy \sin 2\phi}{r^2} \right) y \right] \end{aligned} \quad (35)$$

where the unit vector $\hat{\mathbf{n}}$ makes an angle ϕ with the x-axis. Taking derivatives of the displacement field

$$\begin{aligned} \frac{\partial u_\alpha^c}{\partial X_\beta} &= \frac{(\zeta_n - \zeta_k)(\lambda + \mu)}{4(\lambda + 2\mu)} \left(\frac{a^2}{r^2} \right) \left[2 \frac{(\zeta_n + \zeta_k)}{(\zeta_n - \zeta_k)} \left(\delta_{\alpha\beta} - 2 \frac{X_\alpha X_\beta}{r^2} \right) \right. \\ &\quad - 4 \left(\frac{\mu}{\lambda + \mu} + \frac{a^2}{r^2} \right) \left(2(\hat{\mathbf{n}} \cdot \hat{\mathbf{r}})\hat{n}_\alpha - \frac{X_\alpha}{r} \right) \frac{X_\beta}{r} \\ &\quad + \left(\frac{2\mu}{\lambda + \mu} + \frac{a^2}{r^2} \right) (2\hat{n}_\alpha \hat{n}_\beta - \delta_{\alpha\beta}) - 4 \left(1 - 2 \frac{a^2}{r^2} \right) (2(\hat{\mathbf{n}} \cdot \hat{\mathbf{r}})^2 - 1) \frac{X_\alpha X_\beta}{r^2} \\ &\quad \left. + 8 \left(1 - \frac{a^2}{r^2} \right) \left((\hat{\mathbf{n}} \cdot \hat{\mathbf{r}})\hat{n}_\beta - (\hat{\mathbf{n}} \cdot \hat{\mathbf{r}})^2 \frac{X_\beta}{r} \right) \frac{X_\alpha}{r} + 2 \left(1 - \frac{a^2}{r^2} \right) (2(\hat{\mathbf{n}} \cdot \hat{\mathbf{r}})^2 - 1) \delta_{\alpha\beta} \right] \end{aligned} \quad (36)$$

and

$$\begin{aligned}
\frac{\partial u_\beta^c}{\partial X_\alpha} &= \frac{(\zeta_n - \zeta_k)(\lambda + \mu)}{4(\lambda + 2\mu)} \left(\frac{a^2}{r^2} \right) \left[2 \frac{(\zeta_n + \zeta_k)}{(\zeta_n - \zeta_k)} \left(\delta_{\alpha\beta} - 2 \frac{X_\alpha X_\beta}{r^2} \right) \right. \\
&\quad - 4 \left(\frac{\mu}{\lambda + \mu} + \frac{a^2}{r^2} \right) \left(2(\hat{\mathbf{n}} \cdot \hat{\mathbf{r}}) \hat{n}_\beta - \frac{X_\beta}{r} \right) \frac{X_\alpha}{r} \\
&\quad + \left(\frac{2\mu}{\lambda + \mu} + \frac{a^2}{r^2} \right) \left(2\hat{n}_\alpha \hat{n}_\beta - \delta_{\alpha\beta} \right) - 4 \left(1 - 2 \frac{a^2}{r^2} \right) \left(2(\hat{\mathbf{n}} \cdot \hat{\mathbf{r}})^2 - 1 \right) \frac{X_\alpha X_\beta}{r^2} \\
&\quad \left. + 8 \left(1 - \frac{a^2}{r^2} \right) \left((\hat{\mathbf{n}} \cdot \hat{\mathbf{r}}) \hat{n}_\alpha - (\hat{\mathbf{n}} \cdot \hat{\mathbf{r}})^2 \frac{X_\alpha}{r} \right) \frac{X_\beta}{r} + 2 \left(1 - \frac{a^2}{r^2} \right) \left(2(\hat{\mathbf{n}} \cdot \hat{\mathbf{r}})^2 - 1 \right) \delta_{\alpha\beta} \right] \quad (37)
\end{aligned}$$

The constrained strain in the matrix can be written as

$$\epsilon_{\alpha\beta}^c = \frac{1}{2} \left(\frac{\partial u_\alpha^c}{\partial X_\beta} + \frac{\partial u_\beta^c}{\partial X_\alpha} \right) \quad (38)$$

Using equations (36) and (37), Eq. (38) becomes

$$\begin{aligned}
\epsilon_{\alpha\beta}^c(\mathbf{X}) &= \frac{(\zeta_n - \zeta_k)(\lambda + \mu)}{4(\lambda + 2\mu)} \left(\frac{a^2}{r^2} \right) \left[2 \frac{(\zeta_n + \zeta_k)}{(\zeta_n - \zeta_k)} \left(\delta_{\alpha\beta} - 2 \frac{X_\alpha X_\beta}{r^2} \right) - 4 \left(\frac{\mu}{\lambda + \mu} + \frac{a^2}{r^2} \right) \left\{ (\hat{\mathbf{n}} \cdot \hat{\mathbf{r}}) \left(\frac{\hat{n}_\alpha X_\beta}{r} + \frac{\hat{n}_\beta X_\alpha}{r} \right) - \frac{X_\alpha X_\beta}{r^2} \right\} \right. \\
&\quad + \left(\frac{2\mu}{\lambda + \mu} + \frac{a^2}{r^2} \right) \left(2\hat{n}_\alpha \hat{n}_\beta - \delta_{\alpha\beta} \right) - 4 \left(1 - 2 \frac{a^2}{r^2} \right) \left(2(\hat{\mathbf{n}} \cdot \hat{\mathbf{r}})^2 - 1 \right) \frac{X_\alpha X_\beta}{r^2} \\
&\quad \left. + 4 \left(1 - \frac{a^2}{r^2} \right) \left\{ (\hat{\mathbf{n}} \cdot \hat{\mathbf{r}}) \left(\frac{\hat{n}_\beta X_\alpha}{r} + \frac{\hat{n}_\alpha X_\beta}{r} \right) - 2(\hat{\mathbf{n}} \cdot \hat{\mathbf{r}})^2 \frac{X_\alpha X_\beta}{r^2} \right\} + 2 \left(1 - \frac{a^2}{r^2} \right) \left(2(\hat{\mathbf{n}} \cdot \hat{\mathbf{r}})^2 - 1 \right) \delta_{\alpha\beta} \right] \quad (39)
\end{aligned}$$

It is easy to see that the trace of $\epsilon_{\alpha\beta}^c(\mathbf{X})$ is given as

$$\epsilon_{\eta\eta}^c(\mathbf{X}) = -\frac{(\zeta_n - \zeta_k)\mu}{(\lambda + 2\mu)} \left(\frac{a^2}{r^2} \right) \left(2(\hat{\mathbf{n}} \cdot \hat{\mathbf{r}})^2 - 1 \right) \quad (40)$$

We can now calculate the constrained stress in the elastic matrix due to the deformed Eshelby inclusion. It follows from Hooke's law:

$$\sigma_{\alpha\beta}^c(\mathbf{X}) = 2\mu \epsilon_{\alpha\beta}^c(\mathbf{X}) + \lambda \epsilon_{\eta\eta}^c(\mathbf{X}) \delta_{\alpha\beta} \quad (41)$$

Plugging Eq. (39) in Eq. (41), we get the final expression for the constrained stress

$$\begin{aligned}
\sigma_{\alpha\beta}^c(\mathbf{X}) &= \frac{(\zeta_n - \zeta_k)\mu(\lambda + \mu)}{2(\lambda + 2\mu)} \left(\frac{a^2}{r^2} \right) \left[2 \frac{(\zeta_n + \zeta_k)}{(\zeta_n - \zeta_k)} \left(\delta_{\alpha\beta} - 2 \frac{X_\alpha X_\beta}{r^2} \right) - 4 \left(\frac{\mu}{\lambda + \mu} + \frac{a^2}{r^2} \right) \left\{ (\hat{\mathbf{n}} \cdot \hat{\mathbf{r}}) \left(\frac{\hat{n}_\alpha X_\beta}{r} + \frac{\hat{n}_\beta X_\alpha}{r} \right) - \frac{X_\alpha X_\beta}{r^2} \right\} \right. \\
&\quad + \left(\frac{2\mu}{\lambda + \mu} + \frac{a^2}{r^2} \right) \left(2\hat{n}_\alpha \hat{n}_\beta - \delta_{\alpha\beta} \right) - 4 \left(1 - 2 \frac{a^2}{r^2} \right) \left(2(\hat{\mathbf{n}} \cdot \hat{\mathbf{r}})^2 - 1 \right) \frac{X_\alpha X_\beta}{r^2} \\
&\quad \left. + 4 \left(1 - \frac{a^2}{r^2} \right) \left\{ (\hat{\mathbf{n}} \cdot \hat{\mathbf{r}}) \left(\frac{\hat{n}_\beta X_\alpha}{r} + \frac{\hat{n}_\alpha X_\beta}{r} \right) - 2(\hat{\mathbf{n}} \cdot \hat{\mathbf{r}})^2 \frac{X_\alpha X_\beta}{r^2} \right\} + 2 \left(1 - \frac{a^2}{r^2} \right) \left(2(\hat{\mathbf{n}} \cdot \hat{\mathbf{r}})^2 - 1 \right) \delta_{\alpha\beta} - \frac{2\lambda}{\lambda + \mu} \left(2(\hat{\mathbf{n}} \cdot \hat{\mathbf{r}})^2 - 1 \right) \delta_{\alpha\beta} \right]. \quad (42)
\end{aligned}$$

IV. ENERGY OF \mathcal{N} ESHELBY INCLUSIONS EMBEDDED IN THE MATRIX

The energy of the \mathcal{N} Eshelby inclusions embedded in a linear-elastic matrix m is given by the following expression

$$E = \frac{1}{2} \sum_{i=1}^{\mathcal{N}} \int_{V_0^i} \sigma_{\alpha\beta}^i \epsilon_{\alpha\beta}^i dV + \frac{1}{2} \int_{V - \sum_{i=1}^{\mathcal{N}} V_0^i} \sigma_{\alpha\beta}^m \epsilon_{\alpha\beta}^m dV \quad (43)$$

where the superscript i denotes the index of the inclusion and m denotes the matrix. Eq (43) can be re-written using the definition of the strain $\epsilon_{\alpha\beta} = (1/2)(u_{\alpha,\beta} + u_{\beta,\alpha})$, where $u_{\alpha,\beta} = \frac{\partial u_\alpha}{\partial X_\beta}$:

$$\begin{aligned}
E &= \frac{1}{4} \sum_{i=1}^{\mathcal{N}} \int_{V_0^i} \sigma_{\alpha\beta}^i \left(u_{\alpha,\beta}^i + u_{\beta,\alpha}^i \right) dV \\
&\quad + \frac{1}{4} \int_{V - \sum_{i=1}^{\mathcal{N}} V_0^i} \sigma_{\alpha\beta}^m \left(u_{\alpha,\beta}^m + u_{\beta,\alpha}^m \right) dV \quad (44)
\end{aligned}$$

Using the symmetry of the stress tensor, we obtain

$$E = \frac{1}{2} \sum_{i=1}^N \int_{V_0^i} \sigma_{\alpha\beta}^i u_{\beta,\alpha}^i dV + \frac{1}{2} \int_{V - \sum_{i=1}^N V_0^i} \sigma_{\alpha\beta}^m u_{\beta,\alpha}^m dV \quad (45)$$

If there are no body forces, we also have the identity

$$\sigma_{\alpha\beta} u_{\beta,\alpha} = (\sigma_{\alpha\beta} u_{\beta})_{,\alpha} - \sigma_{\alpha\beta,\alpha} u_{\beta} = (\sigma_{\alpha\beta} u_{\beta})_{,\alpha} \quad (46)$$

Thus we can write Eq. (45) as

$$E = \frac{1}{2} \sum_{i=1}^N \int_{V_0^i} \left(\sigma_{\alpha\beta}^i u_{\beta}^i \right)_{,\alpha} dV + \frac{1}{2} \int_{V - \sum_{i=1}^N V_0^i} \left(\sigma_{\alpha\beta}^m u_{\beta}^m \right)_{,\alpha} dV. \quad (47)$$

Using Gauss's theorem, we convert these volume integrals into area integrals to obtain

$$E = \frac{1}{2} \sum_{i=1}^N \int_{S_0^i} \sigma_{\alpha\beta}^i u_{\beta}^i \hat{n}_{\alpha}^i dS - \sum_{i=1}^N \frac{1}{2} \int_{S_0^i} \sigma_{\alpha\beta}^m u_{\beta}^m \hat{n}_{\alpha}^i dS + \frac{1}{2} \int_{S_{\infty}} \sigma_{\alpha\beta}^m u_{\beta}^m \hat{n}_{\alpha}^{\infty} dS, \quad (48)$$

where \hat{n}^i and \hat{n}^{∞} are unit vectors both pointing outwards from the surfaces bounding the inclusion volume V_0^i and the matrix boundary respectively. Eq. (48) can be re-written as follows

$$\begin{aligned} E &= \frac{1}{2} \int_{S_{\infty}} \sigma_{\alpha\beta}^m u_{\beta}^m dS + \frac{1}{2} \sum_{i=1}^N \int_{S_0^i} \left(\sigma_{\alpha\beta}^i u_{\beta}^i - \sigma_{\alpha\beta}^m u_{\beta}^m \right) \hat{n}_{\alpha}^i dS \\ &= \frac{1}{2} \sigma_{\alpha\beta}^{\infty} \epsilon_{\beta\gamma}^{\infty} \int_{S_{\infty}} X_{\gamma} \hat{n}_{\alpha}^{\infty} dS + \frac{1}{2} \sum_{i=1}^N \int_{S_0^i} \left(\sigma_{\alpha\beta}^i u_{\beta}^i - \sigma_{\alpha\beta}^m u_{\beta}^m \right) \hat{n}_{\alpha}^i dS^{\text{get}} \\ &= \frac{1}{2} \sigma_{\alpha\beta}^{\infty} \epsilon_{\beta\alpha}^{\infty} V + \frac{1}{2} \sum_{i=1}^N \int_{S_0^i} \left(\sigma_{\alpha\beta}^i u_{\beta}^i - \sigma_{\alpha\beta}^m u_{\beta}^m \right) \hat{n}_{\alpha}^i dS \quad (49) \end{aligned}$$

Thus we can re-write Eq. (12) as

$$\begin{aligned} \epsilon_{\alpha\beta}^m(\mathbf{X}) &= \sum_{i=1}^N \epsilon_{\alpha\beta}^{c,i}(\mathbf{X}) + \epsilon_{\alpha\beta}^{\infty} \\ \sigma_{\alpha\beta}^m(\mathbf{X}) &= \sum_{i=1}^N \sigma_{\alpha\beta}^{c,i}(\mathbf{X}) + \sigma_{\alpha\beta}^{\infty} \\ u_{\alpha\beta}^m(\mathbf{X}) &= \sum_{i=1}^N u_{\alpha\beta}^{c,i}(\mathbf{X}) + u_{\alpha\beta}^{\infty} \quad (50) \end{aligned}$$

where $\epsilon_{\alpha\beta}^{c,i}(\mathbf{X})$ denotes the constrained strain at \mathbf{X} in the matrix due to the i^{th} Eshelby inclusion. We also have for locations \mathbf{X} inside the inclusions

$$\begin{aligned} \epsilon_{\alpha\beta}^i(\mathbf{X}) &= \sum_{j \neq i} \epsilon_{\alpha\beta}^{c,j}(\mathbf{X}) + \epsilon_{\alpha\beta}^{c,i}(\mathbf{X}) - \epsilon_{\alpha\beta}^{*,i} + \epsilon_{\alpha\beta}^{\infty} \\ \sigma_{\alpha\beta}^i(\mathbf{X}) &= \sum_{j \neq i} \sigma_{\alpha\beta}^{c,j}(\mathbf{X}) + \sigma_{\alpha\beta}^{c,i}(\mathbf{X}) - \sigma_{\alpha\beta}^{*,i} + \sigma_{\alpha\beta}^{\infty} \\ u_{\alpha}^i(\mathbf{X}) &= \sum_{j \neq i} u_{\alpha}^{c,j}(\mathbf{X}) + u_{\alpha}^{c,i}(\mathbf{X}) - \epsilon_{\alpha\beta}^{*,i} X_{\beta} + u_{\alpha}^{\infty} \quad (51) \end{aligned}$$

where $\epsilon_{\alpha\beta}^{*,i}$ is the eigen-strain of the i^{th} Eshelby inclusion and so on. Note that in the expression for the strain in the inclusion given by Eq. (51), we have subtracted the contribution of eigen-strain from the constrained strain leaving only the elastic contribution to calculate correctly the elastic contribution to the energy. Using these expressions, the elastic energy of the system can be written from Eq. (49) as follows:

$$E = \frac{1}{2} \sigma_{\alpha\beta}^{\infty} \epsilon_{\beta\alpha}^{\infty} V + \frac{1}{2} \sum_{i=1}^N \int_{S_0^i} \left(\sigma_{\alpha\beta}^i u_{\beta}^i - \sigma_{\alpha\beta}^m u_{\beta}^m \right) \hat{n}_{\alpha}^i dS \quad (52)$$

Since the traction force has to be continuous at the inclusion boundary (Newton's IIIrd law), we have

$$\sigma_{\alpha\beta}^i \hat{n}_{\alpha}^i = \sigma_{\alpha\beta}^m \hat{n}_{\alpha}^i \quad (53)$$

which gives us from Eq. (52),

$$E = \frac{1}{2} \sigma_{\alpha\beta}^{\infty} \epsilon_{\alpha\beta}^{\infty} V + \frac{1}{2} \sum_{i=1}^N \int_{S_0^i} \sigma_{\alpha\beta}^i \hat{n}_{\alpha}^i (u_{\beta}^i - u_{\beta}^m) dS \quad (54)$$

We also have from equations (50) and (51)

$$u_{\beta}^i - u_{\beta}^m = -\epsilon_{\beta\xi}^{*,i} X_{\xi} \quad (55)$$

On plugging this expression into Eq. (54) we finally

$$\begin{aligned} E &= \frac{1}{2} \sigma_{\alpha\beta}^{\infty} \epsilon_{\alpha\beta}^{\infty} V - \frac{1}{2} \sum_{i=1}^N \int_{S_0^i} \sigma_{\alpha\beta}^i \hat{n}_{\alpha}^i \epsilon_{\beta\xi}^{*,i} X_{\xi} dS \\ &= \frac{1}{2} \sigma_{\alpha\beta}^{\infty} \epsilon_{\alpha\beta}^{\infty} V - \frac{1}{2} \sum_{i=1}^N \epsilon_{\beta\xi}^{*,i} \int_{V_0^i} \left(\sigma_{\alpha\beta}^i X_{\xi} \right)_{,\alpha} dV \\ &= \frac{1}{2} \sigma_{\alpha\beta}^{\infty} \epsilon_{\alpha\beta}^{\infty} V - \frac{1}{2} \sum_{i=1}^N \epsilon_{\beta\xi}^{*,i} \int_{V_0^i} \sigma_{\alpha\beta}^i \delta_{\xi\alpha} dV \\ &= \frac{1}{2} \sigma_{\alpha\beta}^{\infty} \epsilon_{\alpha\beta}^{\infty} V - \frac{1}{2} \sum_{i=1}^N \overline{V_0^i \epsilon_{\beta\alpha}^{*,i} \sigma_{\alpha\beta}^i} \quad (56) \end{aligned}$$

where $\overline{\sigma_{\alpha\beta}^i} \equiv (1/V_0^i) \int_{V_0^i} \sigma_{\alpha\beta}^i dV$. Using the expression for $\sigma_{\alpha\beta}^i$ from equation Eq.(51), we obtain

$$\overline{\sigma_{\alpha\beta}^i} = \sigma_{\alpha\beta}^{\infty} + \sum_{j \neq i} \sigma_{\alpha\beta}^{c,j}(r^{ij}) + \sigma_{\alpha\beta}^{c,i}(r^{ij}) - \sigma_{\alpha\beta}^{*,i} \quad (57)$$

Eq. (57) is a far field approximation which assumes that $r^{ij} \gg a$. As $r^{ij} \rightarrow a$, clearly the spatial integrals contributing to $\overline{\sigma_{\alpha\beta}^i}$ must be computed explicitly and cannot be replaced by the single distance r^{ij} between the centers of the Eshelby inclusions i and j .

Using equations (56) and (57), we can write down the final form of the elastic energy expression.

$$\begin{aligned}
E &= \frac{1}{2}\sigma_{\alpha\beta}^{\infty}\epsilon_{\alpha\beta}^{\infty}V - \frac{1}{2}\sigma_{\alpha\beta}^{\infty}\sum_{i=1}^N\epsilon_{\beta\alpha}^{*,i}V_0^i - \frac{1}{2}\sum_{i=1}^N\epsilon_{\beta\alpha}^{*,i}\sigma_{\alpha\beta}^{c,i}V_0^i \\
&+ \frac{1}{2}\sum_{i=1}^N\epsilon_{\beta\alpha}^{*,i}\sigma_{\alpha\beta}^{*,i}V_0^i - \frac{1}{2}\sum_{i=1}^N\epsilon_{\beta\alpha}^{*,i}V_0^i\sum_{j\neq i}\sigma_{\alpha\beta}^{c,j}(r^{ij}) \\
&= E_{mat} + E_{\infty} + E_{esh} + E_{inc}
\end{aligned} \tag{58}$$

where each component of energy is defined as

$$\begin{aligned}
E_{mat} &= \frac{1}{2}\sigma_{\alpha\beta}^{\infty}\epsilon_{\beta\alpha}^{\infty}V \\
E_{\infty} &= -\frac{1}{2}\sigma_{\alpha\beta}^{\infty}\sum_{i=1}^N\epsilon_{\beta\alpha}^{*,i}V_0^i \\
E_{esh} &= \frac{1}{2}\sum_{i=1}^N(\sigma_{\alpha\beta}^{*,i} - \sigma_{\alpha\beta}^{c,i})\epsilon_{\beta\alpha}^{*,i}V_0^i \\
E_{inc} &= -\frac{1}{2}\sum_{i=1}^N\epsilon_{\beta\alpha}^{*,i}V_0^i\sum_{j\neq i}\sigma_{\alpha\beta}^{c,j}(r^{ij})
\end{aligned} \tag{59}$$

Here the eigen-strain $\epsilon_{\alpha\beta}^{*,i}$ and volume V_0^i associated with any i^{th} Eshelby inclusion are given as

$$\begin{aligned}
V_0^i &= \frac{\pi a^2}{2} \\
\epsilon_{\alpha\beta}^{*,i} &= \frac{(\zeta_n - \zeta_k)}{2}(2\hat{n}_{\alpha}^i\hat{n}_{\beta}^i - \delta_{\alpha\beta}) + \frac{(\zeta_n + \zeta_k)}{2}\delta_{\alpha\beta}
\end{aligned} \tag{60}$$

Also for a 2D material being loaded under uni-axial strain with free boundaries along \hat{y} , we can write the form of the global stress tensor as

$$\sigma^{\infty} = \begin{pmatrix} \sigma_{xx}^{\infty} & 0 \\ 0 & 0 \end{pmatrix} \tag{61}$$

By Hooke's law, we get the expression for applied global stress tensor

$$\sigma_{\alpha\beta}^{\infty} = 2\mu\epsilon_{\alpha\beta}^{\infty} + \lambda\epsilon_{\eta\eta}^{\infty}\delta_{\alpha\beta} \tag{62}$$

Taking trace of Eq. (62), we find

$$\epsilon_{\eta\eta}^{\infty} = \frac{1}{2(\lambda + \mu)}\sigma_{\eta\eta}^{\infty} = \frac{1}{2(\lambda + \mu)}\sigma_{xx}^{\infty} \tag{63}$$

Plugging Eq. (63) in Eq. (62), we find

$$\sigma_{xx}^{\infty} = \frac{4\mu(\lambda + \mu)\gamma}{\lambda + 2\mu} \tag{64}$$

where γ is the external strain. In the following, we discuss these components of elastic energy as shown in Eq. (59) in detail:

E_{mat} : It is the elastic energy that would be present in the strained matrix in the absence of inclusions. Plugging

equation (61) and (64) into Eq. (59), we get the following expression

$$E_{mat} = \frac{2\mu(\lambda + \mu)\gamma^2V}{\lambda + 2\mu} \tag{65}$$

E_{∞} : It is the contribution to the elastic energy caused by the Eshelby inclusions themselves. Note that this term can make a negative contribution with respect to E_{mat} . Again plugging equations (61), (64) and (60) into Eq. (59), we find

$$\begin{aligned}
E_{\infty} &= \frac{-2\pi a^2\mu(\lambda + \mu)\gamma}{(\lambda + 2\mu)}\sum_{i=1}^N\left\{\frac{(\zeta_n - \zeta_k)}{2}(2(\hat{n}_x^i)^2 - 1) \right. \\
&\quad \left. + \frac{(\zeta_n + \zeta_k)}{2}\right\}
\end{aligned} \tag{66}$$

To find the orientation of each Eshelby inclusion with respect to the principal stress direction, we need to minimize E_{∞} with respect to θ , where $\theta = \cos^{-1}(n_x^i) = \sin^{-1}(n_y^i)$. We thus get

$$\begin{aligned}
\frac{d}{d\theta}\left(\frac{(\zeta_n - \zeta_k)}{2}(2\cos^2\theta - 1) + \frac{(\zeta_n + \zeta_k)}{2}\right) &= 0 \\
\theta = 0 \quad \text{or} \quad \frac{\pi}{2}
\end{aligned} \tag{67}$$

Hence each Eshelby inclusion must be oriented along the principal stress direction (or $\theta = 0$).

E_{esh} : It is the self energy required to create the Eshelby inclusion and it is always positive. To calculate this term, we need the following quantities:

$$\begin{aligned}
\sigma_{\alpha\beta}^{c,i} &= C_{\alpha\beta\gamma\delta}\epsilon_{\gamma\delta}^{c,i} \\
&= C_{\alpha\beta\gamma\delta}\mathcal{S}_{\gamma\delta kl}\epsilon_{kl}^{*,i} \\
&= \frac{(\lambda + \mu)}{2(\lambda + 2\mu)}\left[2(\zeta_n + \zeta_k)(\lambda + \mu)\delta_{\alpha\beta} \right. \\
&\quad \left. + \frac{\mu(\lambda + 3\mu)(\zeta_n - \zeta_k)}{(\lambda + \mu)}(2\hat{n}_{\alpha}^i\hat{n}_{\beta}^i - \delta_{\alpha\beta})\right]
\end{aligned} \tag{68}$$

In deriving Eq. (68), we have used equations (10), (5) and (6). The eigen stress for the i^{th} Eshelby inclusion can be written [using Eq. (9)] as

$$\sigma_{\alpha\beta}^{*,i} = (\lambda + \mu)(\zeta_n + \zeta_k)\delta_{\alpha\beta} + \mu(\zeta_n - \zeta_k)(2\hat{n}_{\alpha}^i\hat{n}_{\beta}^i - \delta_{\alpha\beta}) \tag{69}$$

Combining this and the expression for eigen-strain from Eq. (60), Eq. (59) becomes

$$\begin{aligned}
E_{esh} &= \frac{\pi a^2}{2}\sum_{i=1}^N(\sigma_{\alpha\beta}^{*,i} - \sigma_{\alpha\beta}^{c,i})\epsilon_{\beta\alpha}^{*,i} \\
&= \frac{\pi a^2\mathcal{N}\mu(\lambda + \mu)}{4(\lambda + 2\mu)}\{2(\zeta_n + \zeta_k)^2 + (\zeta_n - \zeta_k)^2\}
\end{aligned} \tag{70}$$

E_{inc} : This term arises due to the interaction between Eshelby inclusions in the ‘‘far field approximation’’. We

note from Eq. (59)

$$\begin{aligned}
E_{inc} &= -\frac{1}{2} \sum_{i=1}^N \epsilon_{\alpha\beta}^{*,i} V_0^i \sum_{j \neq i} \sigma_{\alpha\beta}^{c,j}(\mathbf{r}^{ij}) \\
&= -\frac{\pi a^2}{2} \sum_{\langle ij \rangle} \left\{ \epsilon_{\beta\alpha}^{*,i} \sigma_{\alpha\beta}^{c,j}(\mathbf{r}^{ij}) + \epsilon_{\beta\alpha}^{*,j} \sigma_{\alpha\beta}^{c,i}(\mathbf{r}^{ij}) \right\} \quad (71)
\end{aligned}$$

Recalling the value of eigen-strain (Eq. (3)) and constrained stress (Eq. (42)) due to an i^{th} Eshelby inclusion, we write down Eq. (71) (after simplifying):

$$\begin{aligned}
E_{inc} &= -2\pi a^2 \sum_{\langle ij \rangle} \frac{\mu(\lambda + \mu)}{(\lambda + 2\mu)} \left(\frac{a^2}{r^{ij^2}} \right) \left[(\zeta_k^2 - \zeta_n^2) \left((\hat{\mathbf{n}}^i \cdot \hat{\mathbf{r}}^{ij})^2 + (\hat{\mathbf{n}}^j \cdot \hat{\mathbf{r}}^{ij})^2 - 1 \right) + \right. \\
&\quad \frac{(\zeta_n - \zeta_k)^2}{8} \left\{ -4 \left(\frac{\mu}{\lambda + \mu} + \frac{a^2}{r^{ij^2}} \right) \left(4(\hat{\mathbf{n}}^i \cdot \hat{\mathbf{n}}^j)(\hat{\mathbf{n}}^i \cdot \hat{\mathbf{r}}^{ij})(\hat{\mathbf{n}}^j \cdot \hat{\mathbf{r}}^{ij}) - 2(\hat{\mathbf{n}}^i \cdot \hat{\mathbf{r}}^{ij})^2 - 2(\hat{\mathbf{n}}^j \cdot \hat{\mathbf{r}}^{ij})^2 + 1 \right) \right. \\
&\quad + 2 \left(\frac{2\mu}{\lambda + \mu} + \frac{a^2}{r^{ij^2}} \right) \left(2(\hat{\mathbf{n}}^i \cdot \hat{\mathbf{n}}^j)^2 - 1 \right) - 4 \left(1 - 2 \frac{a^2}{r^{ij^2}} \right) \left(2(\hat{\mathbf{n}}^i \cdot \hat{\mathbf{r}}^{ij})^2 - 1 \right) \left(2(\hat{\mathbf{n}}^j \cdot \hat{\mathbf{r}}^{ij})^2 - 1 \right) \\
&\quad \left. \left. + 16 \left(1 - \frac{a^2}{r^{ij^2}} \right) \left((\hat{\mathbf{n}}^i \cdot \hat{\mathbf{n}}^j)(\hat{\mathbf{n}}^i \cdot \hat{\mathbf{r}}^{ij})(\hat{\mathbf{n}}^j \cdot \hat{\mathbf{r}}^{ij}) - (\hat{\mathbf{n}}^i \cdot \hat{\mathbf{r}}^{ij})^2 (\hat{\mathbf{n}}^j \cdot \hat{\mathbf{r}}^{ij})^2 \right) \right\} \right] \quad (72)
\end{aligned}$$

In deriving Eq. (72), we have used the following identities:

$$\begin{aligned}
\epsilon_{\alpha\beta}^{*,i} \left(\delta_{\alpha\beta} - 2 \frac{X_{\alpha}^{ij} X_{\beta}^{ij}}{r^{ij^2}} \right) &= (\zeta_n - \zeta_k) \left(1 - 2(\hat{\mathbf{n}}^i \cdot \hat{\mathbf{r}}^{ij})^2 \right) \\
\epsilon_{\alpha\beta}^{*,i} \left[(\hat{\mathbf{n}}^j \cdot \hat{\mathbf{r}}^{ij}) \left(\frac{\hat{n}_{\alpha}^j X_{\beta}^{ij}}{r^{ij}} + \frac{\hat{n}_{\beta}^j X_{\alpha}^{ij}}{r^{ij}} \right) - \frac{X_{\alpha}^{ij} X_{\beta}^{ij}}{r^{ij^2}} \right] &= (\zeta_n + \zeta_k) \left((\hat{\mathbf{n}}^j \cdot \hat{\mathbf{r}}^{ij})^2 - \frac{1}{2} \right) + \\
(\zeta_n - \zeta_k) \left(2(\hat{\mathbf{n}}^i \cdot \hat{\mathbf{n}}^j)(\hat{\mathbf{n}}^i \cdot \hat{\mathbf{r}}^{ij})(\hat{\mathbf{n}}^j \cdot \hat{\mathbf{r}}^{ij}) - (\hat{\mathbf{n}}^i \cdot \hat{\mathbf{r}}^{ij})^2 - (\hat{\mathbf{n}}^j \cdot \hat{\mathbf{r}}^{ij})^2 + \frac{1}{2} \right) & \\
\epsilon_{\alpha\beta}^{*,i} (2\hat{n}_{\alpha}^j \hat{n}_{\beta}^j - \delta_{\alpha\beta}) &= (\zeta_n - \zeta_k) \left(2(\hat{\mathbf{n}}^i \cdot \hat{\mathbf{n}}^j)^2 - 1 \right) \\
\epsilon_{\alpha\beta}^{*,i} \frac{X_{\alpha}^{ij} X_{\beta}^{ij}}{r^{ij^2}} &= \frac{(\zeta_n + \zeta_k)}{2} + \frac{(\zeta_n - \zeta_k)}{2} \left(2(\hat{\mathbf{n}}^i \cdot \hat{\mathbf{r}}^{ij})^2 - 1 \right) \\
\epsilon_{\alpha\beta}^{*,i} \left[(\hat{\mathbf{n}}^j \cdot \hat{\mathbf{r}}^{ij}) \left(\frac{\hat{n}_{\alpha}^j X_{\beta}^{ij}}{r^{ij}} + \frac{\hat{n}_{\beta}^j X_{\alpha}^{ij}}{r^{ij}} \right) - 2(\hat{\mathbf{n}}^j \cdot \hat{\mathbf{r}}^{ij})^2 \frac{X_{\alpha}^{ij} X_{\beta}^{ij}}{r^{ij^2}} \right] &= 2(\zeta_n - \zeta_k) \left((\hat{\mathbf{n}}^i \cdot \hat{\mathbf{n}}^j)(\hat{\mathbf{n}}^i \cdot \hat{\mathbf{r}}^{ij})(\hat{\mathbf{n}}^j \cdot \hat{\mathbf{r}}^{ij}) \right. \\
&\quad \left. - (\hat{\mathbf{n}}^i \cdot \hat{\mathbf{r}}^{ij})^2 (\hat{\mathbf{n}}^j \cdot \hat{\mathbf{r}}^{ij})^2 \right) \\
\epsilon_{\alpha\beta}^{*,i} \delta_{\alpha\beta} &= (\zeta_n + \zeta_k) \quad (73)
\end{aligned}$$

To calculate the shear band angle with respect to the principal direction of strain, we have to minimize E_{inc} with respect to θ . Assuming all eigen directions to be the same, i.e taking $\hat{\mathbf{n}}^i = \hat{\mathbf{n}}^j = \hat{\mathbf{n}}$, $(\hat{\mathbf{n}} \cdot \hat{\mathbf{r}}^{ij})^2 = \cos^2 \theta = \chi$ and $\frac{a^2}{r^{ij^2}} \rightarrow 0$ (far field approximation) we find, by putting $\frac{d}{d\chi} E_{inc} = 0$:

$$\begin{aligned}
\chi &= \frac{1}{2} - \frac{1}{4} \frac{(\zeta_n + \zeta_k)}{(\zeta_n - \zeta_k)} \\
\text{or} & \\
\theta &= \cos^{-1} \sqrt{\frac{1}{2} - \frac{1}{4} \frac{(\zeta_n + \zeta_k)}{(\zeta_n - \zeta_k)}} \quad (74)
\end{aligned}$$

It is very easy to see from Eq. (74) that the area preserving case, such as pure shear implies $\zeta_n = -\zeta_k$ leading to the angle exactly equal to 45° . As can be expected,

other loading conditions may result in different values of the angle. The two extreme cases occur for $|\zeta_n/\zeta_k| \rightarrow 0$ and $|\zeta_n/\zeta_k| \rightarrow \infty$. The first case corresponds to an angle of 30° and the second - to an angle of 60° . Therefore all experimental observations should fall between these two extreme universal limits. Following Ref.[8], we find that indeed all the experimental data presented there fall within our theoretical limits. We return now to our simulations shown in Fig. 1 to rationalize the angles observed. In order to understand the angles observed in our simulations we need to figure how different loading conditions affect the values of ζ_n and ζ_k . We find that in the case of extension [see Fig (4)], the outward displacement significantly dominates the inward displacement, realizing a higher ratio of $|\zeta_n/\zeta_k|$ as compared to the case of compression [see Fig. (5)].

We attribute this asymmetry to the steeper rise in the repulsive core as compared to the weakly attractive tail in any generic inter-particle interaction potentials. To estimate the ratio $|\zeta_n/\zeta_k|$, we first calculate average length of both the incoming and the outgoing vectors in a small region around the core of the plastic event. The ratio of these lengths then determines $|\zeta_n/\zeta_k|$. For compression, we find that $|\zeta_n/\zeta_k| \approx 1.15$ and for extension, we find $|\zeta_n/\zeta_k| \approx 4.05$. Plugging these values in Eq. (74), we find the shear band angle of 46° for the compression and 54° - for the extension; both are in very good agreement with the angles observed in the simulations presented in Fig. (1). In the following section, we explain how the present atomistic theory can predict the yield strain under such loading conditions.

V. PREDICTING YIELD STRAIN

In terms of our atomistic model, the global yield becomes possible if the formation of infinitely many Eshelby inclusions is energetically favorable (in the thermodynamic limit). In other words, the system should be able to create a density $\rho \equiv \mathcal{N}/L$ of such inclusions where L is the global linear scale of the system. Assuming all eigen strains and the eigen directions to be the same, we have from equations (66) and (70),

$$E_\infty = \frac{-2\pi a^2 \mu (\lambda + \mu) \gamma \zeta_n \mathcal{N}}{(\lambda + 2\mu)}, \quad (75)$$

and

$$E_{esh} = \frac{\pi a^2 \mu (\lambda + \mu)}{4(\lambda + 2\mu)} \{2(\zeta_n + \zeta_k)^2 + (\zeta_n - \zeta_k)^2\} \mathcal{N}. \quad (76)$$

Since the inclusions are localized in a strip of dimensions La , the energy density of these two terms is computed as

$$\begin{aligned} \frac{E_\infty + E_{esh}}{La} &= \frac{-2\pi a \mu (\lambda + \mu) \gamma \zeta_n}{(\lambda + 2\mu)} \rho \\ &+ \frac{\pi a^2 \mu (\lambda + \mu)}{4(\lambda + 2\mu)} \{2(\zeta_n + \zeta_k)^2 + (\zeta_n - \zeta_k)^2\} \rho. \end{aligned} \quad (77)$$

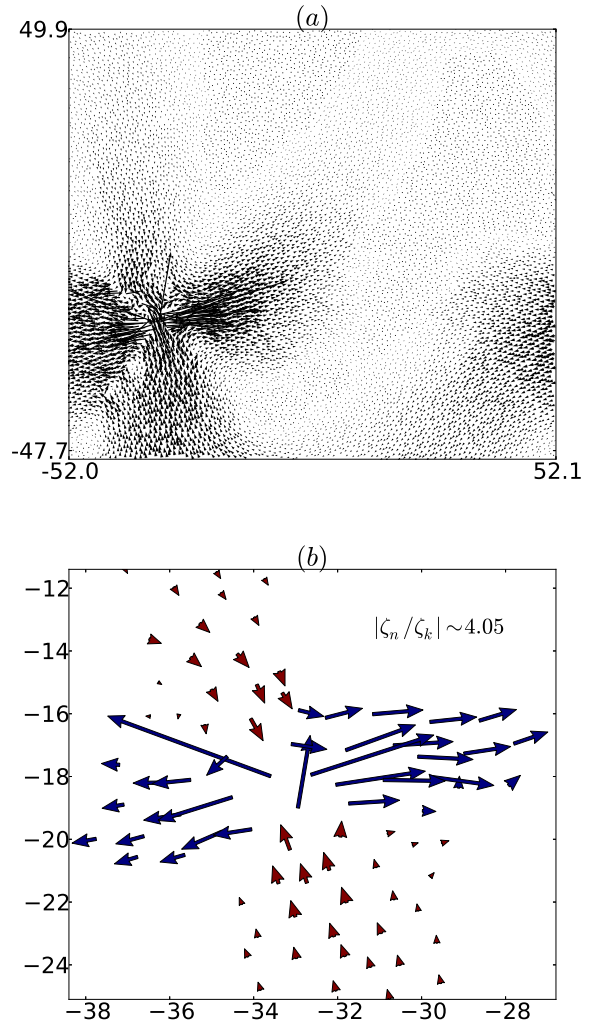


FIG. 4. (a) A fundamental plastic event during an AQS uniaxial extension simulation of a 2-dimensional amorphous solid. Shown is the non-affine displacement field in the whole system. (b) a small region around the core of the event shown in (a). Again for clarity we show only the incoming and outgoing arrows. The ratio $\frac{\zeta_n}{\zeta_k} \approx 4.05$ is determined by the ratio of the average lengths of the outgoing and incoming arrows.

It is easy to check that these two terms are the only ones that are *linear* in the density ρ (other terms are either of order ρ^0 or ρ^2). Now for $\gamma < \gamma_Y$ this energy density *increases* with ρ . The only solution that minimizes the energy is the single inclusion with $\rho = 0$. The condition that identifies γ_Y requires the derivative of this energy density with respect to ρ to vanish. In other words, the coefficient of ρ in Eq. (77) should vanish. Solving for the value of γ that satisfies this condition we find

$$\gamma_Y = \frac{\zeta_n}{4} \left[\left(1 + \frac{\zeta_k}{\zeta_n}\right)^2 + \frac{1}{2} \left(1 - \frac{\zeta_k}{\zeta_n}\right)^2 \right] \quad (78)$$

In order to determine the yield strain we need in ad-

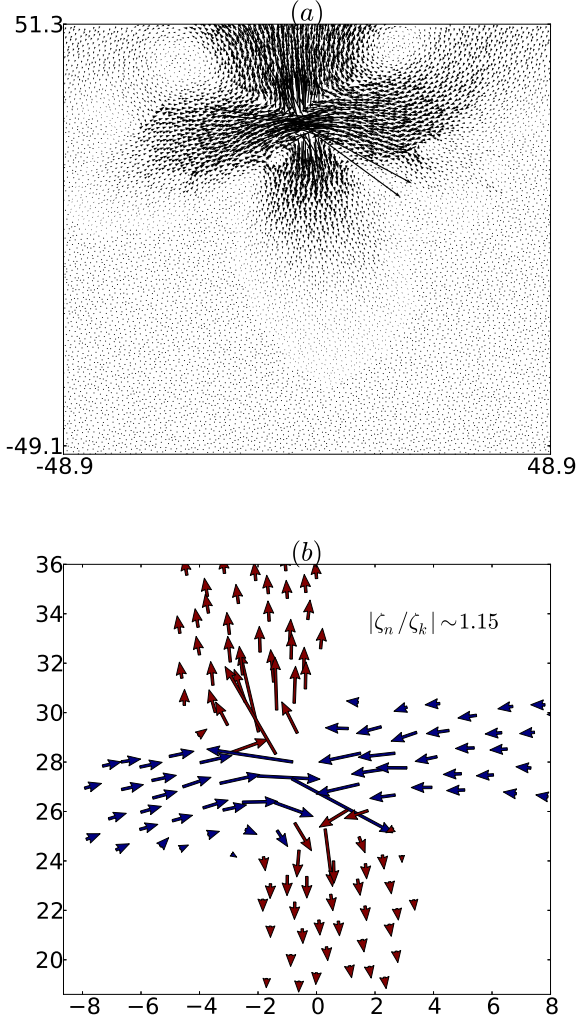


FIG. 5. (a) A fundamental plastic event during an AQS uniaxial compression simulation of a 2-dimensional amorphous solid. Shown is the non-affine displacement field in the whole system. (b) a small region around the core of the event shown in (a). For clarity we show only the incoming and outgoing arrows. The ratio $\frac{\zeta_n}{\zeta_k} \approx 1.15$ is determined by the ratio of the average lengths of the incoming and outgoing arrows.

dition to the ratio ζ_n/ζ_k also the value of ζ_n . To compute the latter value, we find the best fit for the analytic expression of the elastic field produced by the Eshelby quadrupolar structure (Eq. (34)) to our numerical findings. Such a fitting procedure yields the values of (a, ζ_n) as $(0.9, -0.14)$ and $(0.9, 0.09)$ for compression and extension respectively. In Fig (6), we show our fits for both cases.

Using Eq. (78) and the estimates of ζ_n and ζ_n/ζ_k , we estimate the yield strain for the case of compression and

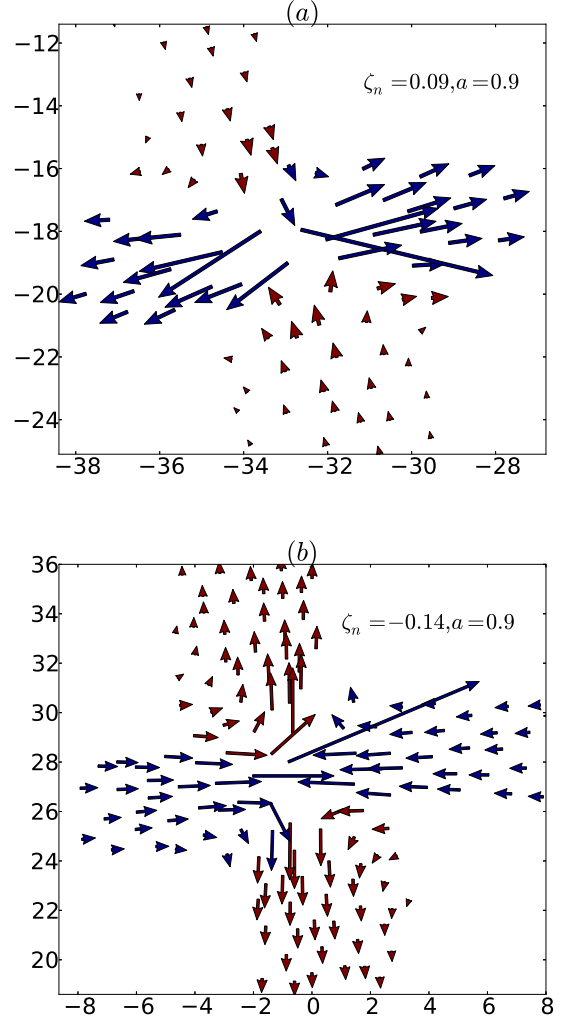


FIG. 6. (a) The fundamental plastic event of Fig. 4b observed during extension is modeled by an Eshelby inclusion. The best fit parameters ia found to be $\zeta_n \approx 0.09, a = 0.9$. (b) The same for the plastic event of Fig. 5b with a best fit given by $\zeta_n \approx -0.14, a = 0.9$.

extension as

$$\begin{aligned} |\gamma_Y| &\approx 6\% , & \text{for compression} \\ |\gamma_Y| &\approx 3\% , & \text{for extension} \end{aligned} \quad (79)$$

This should be compared with the observed values of 5.5% and 3.5% respectively in Fig. (2). We consider the agreement quite satisfactory.

VI. CONCLUSIONS

Experimental observations and numerical simulations show that plastic phenomena in amorphous solids demonstrate essential asymmetry between the cases of uniaxial compression and extension. These asymmetries

are manifested in different angles the shear bands form with respect to the principal direction of stress and in very different values of the yield strain. The results presented in this paper demonstrate that both asymmetries can be quantitatively described on the basis of atomistic theory of plastic events. We also derive analytically that the values of the shear band angles lie between $30^\circ - 60^\circ$ in good agreement with available experimental data. We reiterate the essential steps: one calculated the energy associated with \mathcal{N} Eshelby inclusions, and in view of our athermal conditions minimizes this energy to find the selected distribution of inclusions. We find that for $\gamma < \gamma_Y$ the only solution that minimizes the energy is that containing a single Eshelby inclusion. At $\gamma = \gamma_Y$ a new branch of solutions can open up, allowing for a

density of inclusions to establish itself. The minimum energy is realized by a line of equi-distant inclusions that aligns with and angle θ to the principal stress axis. The angle depends on the loading conditions as encoded by the eigenvalues of the Eshelby quadrupole. Only for simple shear we expect this angle to be 45° , while in general it is limited between 30° and 60° . Finally we computed analytically the yield-strain asymmetry under uniaxial loading conditions. A natural extension of our present work is a 3d generalization. Other possible directions would be to include finite temperature and strain rate effects.

Acknowledgments: this work was supported by the Israel Science Foundation, the German-Israeli Foundation and by the ERC under the STANPAS “ideas” grant.

-
- [1] P.W. Anderson Phys. Rev. (**109**), 1492 (1958)
- [2] R. Dasgupta, H. G. E. Hentschel and I. Procaccia, Phys.Rev. Lett., **109** 255502 (2012).
- [3] R. Dasgupta, O. Gendelman, I. Procaccia and C. Shor “Shear localization in 3-Dimensional Amorphous Solids”, to be submitted to PRE.
- [4] C.E. Maloney and A. Lemaître, Phys. Rev. E **74**, 016118 (2006).
- [5] D. L. Malandro and D. J. Lacks, J. Chem. Phys. **110**, 4593 (1999).
- [6] R. Dasgupta, S. Karmakar and I. Procaccia, Phys. Rev. Lett. **108**, 075701 (2012).
- [7] S. Karmakar, E. Lerner, I. Procaccia, Phys. Rev. E (**82**), 055103(R) (2010)
- [8] For extensive experimental evidence see Y.F. Gao, L. Wang, H. Bei and T.G. Nieh, Acta Materiala, **59**, 4159 (2011), and references therein.
- [9] Ashwin J., O. Gendelman, I. Procaccia and C. Shor “Atomistic theory of the shear band direction in amorphous solids” (PRL Submitted) arXiv:1304.4009v1
- [10] M. Widom, K. J. Strandburg, and R. H. Swendsen, Phys. Rev. Lett. **58**, 706 (1987).
- [11] F. Lancon and L. Billard, J. Phys. France **49**, 249 (1988).
- [12] M. Falk and J. Langer, Phys. Rev. E **57**, 7192 (1998)
- [13] J.W. Rudnicki and J. R. Rice, J. Mech. Phys. Solids, **23**, 371 (1975).
- [14] Rudnicki JW, Olsson WA. Int. J. Rock Mech. Min. Sci. **35**: 4-5, Paper No. 88
- [15] Zhang ZF, Eckert J, Schultz L. Acta Mater (**51**) 1167 (2003).
- [16] M. Zhao and M. Li, Appl. Phys. Lett **93**, 241906 (2008).
- [17] M. Zhao and M. Li, J. Mater. Res. **24**, 2688 (2008).
- [18] J. D. Eshelby, Proc. R. Soc. Lond. A (**241**), 376 (1957).
- [19] J. D. Eshelby, Proc. R. Soc. Lond. A (**252**), 561 (1959).
- [20] C. Weinberger, W. Cai and D. Barnett “Lecture notes, Elasticity and Microscopic Structures” (2004)
- [21] L.D. Landau & E.M. Lifshitz, “Theory of Elasticity” (Volume 7 of A Course of Theoretical Physics), Pergamon Press (1970)